

ANALYSIS OF THE OPERATION OF THE PULSEJET ENGINE

Jon Tegnér¹

¹Affiliation 1

Abstract

Numerical simulations, based on an engine where data can be obtained from the literature, were used to obtain detailed data of the variables in the interior of the engine. Visualization of relevant variables were used to in detail analyze the events going on in a pulsejet. In the simulations propane was used as fuel.

It was found that the efficiency of the operation of the engine was markedly improved when the equivalence ration was reduced from stoichiometric to a lean value of 0.6. The numerical results could be used to provide an understanding of this behavior; it was shown that at stoichiometric conditions a rather large part of the combustion occurred at a pressure below ambient, whereas for the leaner case this “low pressure burning” was reduced to a high degree.

This result compares well with the claim in a thesis from University of Texas, “The synchronous injection ignition valveless pulsejet”, 1987, that an improved strategy for injection and ignition could improve the performance of a pulsejet to equal that of a turbojet. And according to this thesis this improvement should be achieved by forcing the combustion to occur at a more favorable time in the cycle (when the pressure is higher). This particular result was reproduced with a performance model developed in this study.

Keywords: Pulsejet, pulse combustion, visualization, improved performance

1. Introduction

The construction of a generic pulsejet is extremely simple, and does not include any mechanical compression. As a consequence, this type of engine has the advantage of being considerably less expensive than engines of other types. However, the performance of the pulsejet – especially the specific impulse – is lower than that for e.g., a turbojet engine. Furthermore, although the general principle is simple, the physical processes in the engine are extremely complex, and only partially understood. It is important to realize that at the time when the pulsejet was being actively developed the turbojet was emerging as a superior propulsion system, and thereby – in part because of the complex physics – efforts on developing/improving the pulsejet were diminishing. Today we have different/better tools at hand to analyze the events in the interior of the pulsejet, and it is not at all impossible that the increased knowledge/understanding the use of modern CFD can provide, will make it possible to improve e.g., the inferior specific impulse of the pulsejet. It should further be appreciated that – due to the low cost of such systems – a breakthrough in this field would have a profound impact on all those areas where today the systems rely on the much more expensive turbojet engines for propulsion. Furthermore, as is pointed out in [10] the readily available micro electronics of today makes it possible to implement more efficient ways to operate the engine, and in [10] a thorough analysis shows that by implementing a different technique for the injection of the fuel – *the Synchronous Injection Ignition (SSI)* – the performance of the pulsejet *can* be improved to match that of the turbojet. Hence, the major goal of the work presented in this report was to further the understanding of the operation of the pulsejet engine.

The simulations were based on the *Curtis Dyna* design [4] and specifically the commercially manufactured *Hobbyking* variant, also known as “RedHead”. For this engine experimental data can be found in the literature, of which the important parameters are the frequency of the engine, and the peak value of the pressure pulses in the combustor; in [4] 232 Hz and around 1.7 bar were reported.

In the first set of simulations the frequency of the pulsations was way too high, at the same time as peak values of the pressure were too low. One of the advantages of using simulations is that one has access to all variables in the flow field, and in this particular case it was discovered that the temperature in the engine was higher than what could be expected. These initial simulations were done using a stoichiometric mixture of fuel (propane) and air – and since a high temperature yields a high speed of sound, and since this in turn can be an explanation of the elevated frequency – the simulations were redone with reduced equivalence ratios.

The simulations with the leaner mixtures rendered results which better agreed with what could be expected for this engine, and in the sections below a great number of illustrations of the important events in a pulsejet engine are presented.

The simulations in this study showed that a reduction of equivalence ratio – i.e., reducing the amount of fuel in each pulse – actually *improved* the performance (as was seen by the higher peak values of the pressure in the combustor obtained with the reduced equivalence ratio) of the engine. And by comparisons between the pressure and the character of the heat release it was found that in this case it could clearly be explained by a more favorable timing – in relation to the pressure – of the heat release during the cycle.

The simulations also clearly revealed the importance of the shape of the burning surface in the engine. In the beginning of the injection phase of the fuel/air mixture a rather smooth, well defined interface between the reactants and the products was developed. There was some reaction going on at this interface, even at this point in time, when the pressure was below ambient. However, as time progressed the burning surface became increasingly more convoluted, with a dramatically increasing burning surface – and consequently a combustion of increased intensity. This timing is important, and the process described above can explain the behavior seen when the equivalence ratio was reduced; a stoichiometric mixture is in general more reactive, and because of this a larger part of the combustion occurred earlier in the process, when the pressure in the combustor was lower, and thereby leading to less efficient combustion. When a leaner – less reacting – mixture was used the onset of the combustion was instead delayed to a more favorable time in the cycle.

Based on the observations of the behaviour in the engine – notably the initially counter intuitive fact that a reduction in equivalence ratio resulted in an increased performance – led to the insight that the combustion has to be “slow and fast” at the same time (here “slow and fast” are used in a wide sense and covers not only the kinetics of the reactions, but also includes the effects of the actual fluid flow): it has to be slow so that a minimum amount of the fuel is consumed when it is introduced, when the pressure is below ambient, and it has to be fast when it finally burns, at a more favorable pressure. The varying pressure is a consequence of the pulsating combustion, and inertial effects of the gas. However, the levels of the peak pressure are still rather low, and as a consequence of this the only way to achieve efficient combustion is if it occurs as fast as possible. As indicated above, to some extent this can be explained by the different character of the burning surface as time progresses, but it should be realized that even other processes are important, as e.g., the kinetics of the reactions (where the equivalence ratio obviously contributes).

It should also be noted that one salient fact of the pulsejet engine is that – in contrast to many other types of engines – when the fresh, cold fuel/air mixture is injected into the combustor it is filled with hot products from the previous pulse. As mentioned above this represents a challenge in that the reactions should be kept at a minimum until the pressure has increased to a more favorable level. But at the same time the elevated temperatures in the combustor will have a notable effect on the combustion. In the study this was illustrated by studying one dimensional simulations of propagating flames at varying temperature, and it was shown that the flame speed depended on the temperature in an exponential manner (for the range considered). This should not to be understood as a claim that laminar flame propagation is predominant in a pulsejet, but rather as an acknowledgement of the importance a high laminar flame speed has on other important aspects – e.g., folding of the flame, volumetric expansion rate, transition to turbulence – of importance to the combustion process. Besides, even though the flow field inside the pulsejet is extremely complex, the fact that the fresh fuel/air mixture is mixed with hot products makes it plausible that there will be patches in the field where the unburned mixture has a considerably elevated temperature – in which case an high laminar

flame speed is indeed an important characteristic of the process.

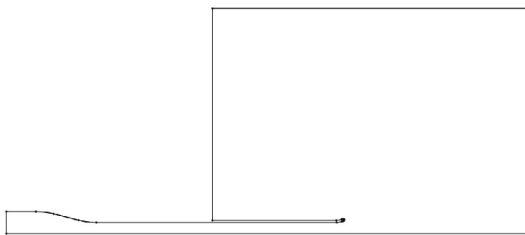
2. Simulation procedure

Numerical simulations based on Reynolds Averaged Navier Stokes (RANS) and in particular Large Eddy Simulation (LES) based techniques combined with accurate combustion chemistry have proved to be a reliable methodology for investigating various combustion applications, [15, 2, 3]. In this study a finite rate chemistry LES combined with a pathway-centric reaction mechanism was used. In this model the filtered transport equations contain filtered source terms representing subgrid stress- and flux-terms, resulting from the effects of the unresolved flow on the resolved flow, and chemical source terms including the filtered reaction-rates from the selected reaction mechanism. The subgrid stress tensor and flux vectors are closed using the Localized Dynamic k-equation Model (LDKM), [8]. The chemical source terms are modeled using the Partially Stirred Reactor (PaSR) model, [9], which is a multi-scale finite-rate chemistry model based on the observation, [11], that turbulent combustion takes place in dispersed fine-structure regions, surrounded by low reaction-rates. The LES-PaSR model equations are solved using a semi-implicit finite-volume code based on the OpenFOAM C++ library, [13]. High-order monotonicity preserving reconstruction of the convective fluxes, central differencing of the inner derivatives of the diffusive fluxes and Crank-Nicholson time-integration provide a second order accurate scheme. The code uses a compressible Pressure-based Implicit Splitting of Operators (PISO) scheme, [1], for the pressure-velocity-density coupling. The chemical source terms are incorporated using an operator-splitting approach, with a Rosenbrock solver, [7], used to solve the resultant stiff ODE system. Stability is enforced using compact stencils and a Courant number < 0.5 . The combustion chemistry employed here is based on the pathway-centric reaction mechanism [14]. All the different details above essentially boils down to a computational method that is capable of handling complex phenomena (e.g., turbulence and combustion) efficiently on rather coarse meshes.

The engine on which the simulations was based on is equipped with ten valves, symmetrically distributed on the front plate, see below for a principal drawing of these features.



In order to take advantage of this symmetry only one tenth of the engine – corresponding to a 36 degree “wedge” of the complete engine was used in the simulations, and the radial and axial extension of the computational domain is shown below (note that in contrast to the drawing above here only half of the engine is shown):



The total length of the engine is 0.48 m, and the lower line in the drawing above represents the center line of the engine (and its extension past the exit of the engine). Note how the computational domain has been extended – both forward and backward, as well as upwards – from the exit of the engine. This is done in order to mitigate problems otherwise at risk to occur as flow structures of different kinds leave the computational domain. As already mentioned, the complete computational domain used in the simulations covered one tenth of the engine, and was essentially obtained by rotating the structure above 36 degrees around the center line of the engine.

The mesh used in the simulations was created using *cfMesh*, and specifically the generator *cartesianMesh* was used. This mesh generator tries to create a mesh where hexahedral cells dominate. *cfMesh* further allows the use of geometrical entities that can be placed in the domain in order to provide higher resolution there. For example, in this case, a rather coarse background mesh was used, and then refinements of different levels were introduced in parts of the domain where a refined resolution was deemed advantageous. In figure 1 the mesh on a slice through the center plane is shown.

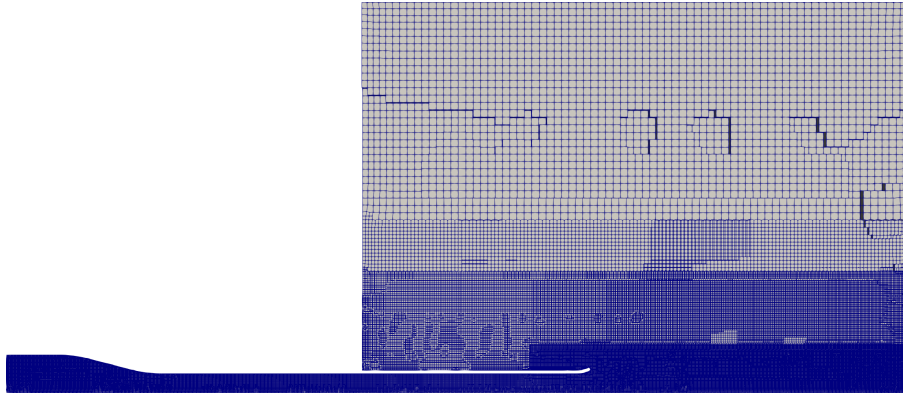


Figure 1 – Illustration of the mesh used in the simulations. Obtained on a slice through the center plane of the domain.

The coarse background mesh can be seen, and the domains with different levels of refinements can also be discerned.

In all the mesh contained about one million cells, of which all but around 13 000 were of the hexahedral type. A higher resolution would be desirable, but since long simulation times are required in order to reach a steady pulsating operation of the engine, simulations on finer mesh were not done in this study.

In the engine under consideration the fuel/air mixture is introduced through *reed valves*, and in order to simplify the numerical treatment of them they are replaced with a specific boundary condition. Here the same as in [4] was used:

$$V_{\text{inflow}} = \begin{cases} 3(p_a - p)/1000 \text{ m/s} & \text{if } p \leq p_a \\ 0 \text{ m/s} & \text{if } p > p_a \end{cases}$$

As boundary conditions on the wall “no-slip” was used for the velocity, and adiabatic was used for the temperature. It is not unlikely that cooling of the walls, as well as heat transfer from the wall to the cold fuel/air mixture when it is introduced in the engine will have some effect, and the present condition is only used since it simplifies the problem.

In the simulations propane was used as fuel, and a three step (Westbrook and Dryer) was used to model the combustion. This is a computationally inexpensive scheme, and although not the most accurate of kinetic schemes it was deemed accurate enough to detect principal traits in the operation of the pulsejet.

In the first simulations the inflow through the inlets was set to be stoichiometric. However, during the work in the study it was found that a better agreement with experiments (frequency of the engine, and peak values on the pressure at the front plate) was obtained when a leaner mixture was used. This in itself is an important observation, and it will be treated in more detail in the next section.

3. Characteristic events in the engine

In order to get the pulsations going the simulations need to be initialized with suitable initial conditions. This does not seem to be overly sensitive, and in this study elevated conditions in the part of the combustor with constant cross sectional area were employed, as indicated in the figure below.



The specific elevated conditions used were: 2000 K and 1.4 bar. Ambient conditions used were: 300 K and 1 bar. In this figure the sliced plane have been mirrored in order to illustrate the complete engine. The main goal of this section is to use the results from the numerical simulations to describe the events occurring in a pulsejet engine, and also illustrate the significant difference in behaviour when the equivalence ratio in the fuel/air mixture was reduced from 1.0 to 0.6.

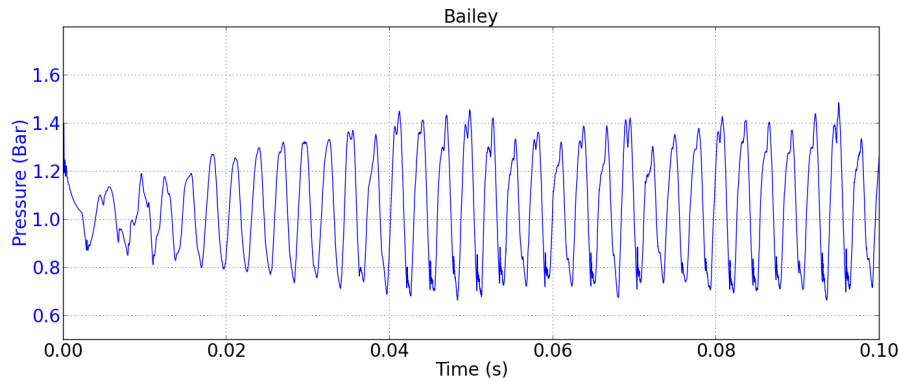


Figure 2 – Results from the initial simulation; pressure at the numerical probe next to the front plate, $\Phi = 1.0$.

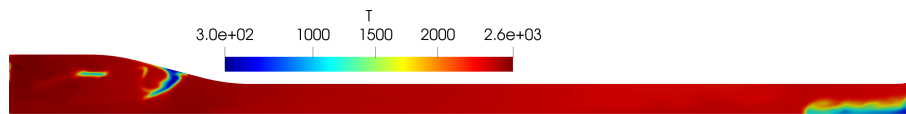


Figure 3 – Color plot of temperature, $\Phi = 1.0$, at $t=0.0951$, when pressure at front plate peaks.

The first set of simulations used a stoichiometric mixture, and the pressure readings from a numerical “probe” placed 1 mm from the front plate, and next to the center line of the engine (i.e., essentially at the lower left corner in the computational domain shown in figure 1) are displayed in figure 2. It can not be seen in the figure (too large time scale), but this pressure curve do show a plateau pressure of 1.4 bar at that probe (for about 0.02 ms, as would have be seen if a different scale were used). The curve also indicates that the chosen initial conditions lead to reasonably stable pulsations after a few pulses. Also noted from the figure is that peak pressure just barely exceeds 1.4 bar (the fact that this corresponds to the initial value should be considered a coincidence). Furthermore, the frequency can be estimated (here this was done by considering the 20 last pulses visible in figure 2) to about 350 Hz. However, this frequency is way too high for the engine under consideration; as indicated in [4] the frequency for this model should instead be around 230 Hz.

When modeling such a complex process as the combustion in a pulsejet there are many things that can be responsible for the frequency being off to such a large degree. However, by studying the different variables in the flow field it was found that the temperature in the engine was very high, as seen in figure 3 values up to 2600 K were reached. Since the speed of sound is proportional to the square of the temperature, and since the frequency by which a pulsejet operates to a high degree depends on the speed of sound it was natural to suspect that the elevated frequency detected could be a consequence of the elevated temperature.

After noticing the very hot interior of the engine, the simulation was restarted from the time dump at $t=0.1$ s from the previous simulation *but* with modified values on the boundary condition modelling the flapper valve. The first simulation used an equivalence number $\Phi = 1.0$ on the fuel/air mixture injected there; in the restarted simulation $\Phi = 0.6$ was instead used.

Since this simulation – with the reduced equivalence ratio – was started with the exact same flow field as the prior simulation, there was bound to be a certain “adjustment period” before a new, stable operation could be developed. For instance, at the beginning of the restarted simulation the temperature in the engine was still unrealistically high.

In figure 4 the pressure readings from the numerical probe at the same position as in the previous case, are displayed. As can be seen there is indeed a transition period, before the pulsations stabilize. When comparing this figure with figure 2 it becomes clear that the amplitude in the case with reduced equivalence ratio is markedly larger. The frequency of the pulsations can – by considering the two last pulses in figure 4 – be estimated to 248 Hz. This is not in complete agreement with the experimentally

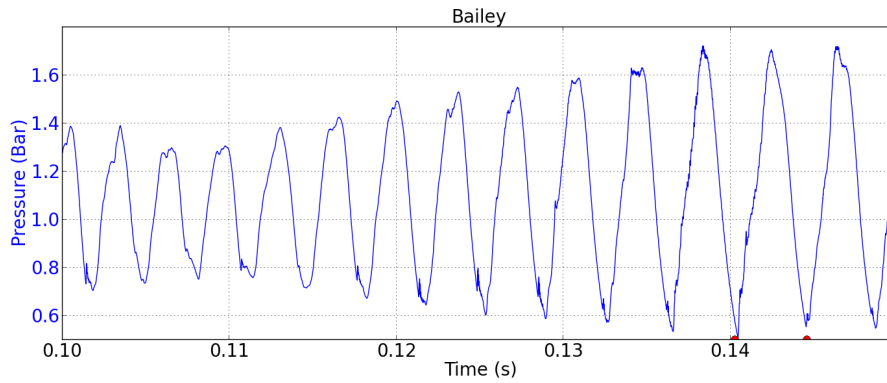


Figure 4 – Pressure readings at numerical probe next to the front plate, with $\Phi = 0.6$.

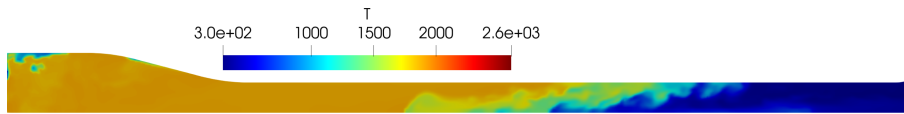


Figure 5 – Color plot of temperature, $\Phi = 0.6$, at $t=0.1425$, when pressure at front plate peaks.

obtained value of the frequency presented in [4], but it is significantly better than that obtained using $\Phi = 1.0$. Furthermore, it is not unreasonable to believe that a better agreement can be obtained through further adjustment of Φ . This was however not pursued in the present study.

In figure 5 the temperature on a plane sliced through the center of the engine is displayed. The same color coding as in figure 3 is used, and it is immediately apparent that the reduction in equivalence ratio leads to a markedly lower temperature in the engine. Something which also substantiates the suspicion that the elevated frequency obtained when $\Phi = 1.0$ can be explained by the elevated sound speed in the engine.

It is also interesting to observe that simulations with the two different equivalence ratios seem to indicate that a higher thrust can be obtained by reducing the amount of fuel supplied to the engine – something which is somewhat counter intuitive. In order to further study this the curves in figure 6 are presented. The blue curves represent the over pressure (bar) at the same numerical probe as introduced above. The red curves represents this over pressure multiplied with a normalized value of the integrated heat release in the whole engine. This variable – the product of the integrated heat release and the over pressure the front plate – will be negative if combustion occurs at a pressure below the ambient value. As can be seen from the curves the case with the stoichiometric mixture has a considerably larger amount of the combustion occurring at a negative over pressure. The higher peak value in the case with $\Phi = 0.6$ also indicate that for this case a larger part of the combustion occurs at a higher pressure, and for this case only a small fraction of the combustion occurs at a pressure below ambient. Hence it becomes obvious that in the case with $\Phi = 0.6$ the inherent compression following the pulsating combustion is better utilized, and it can therefore be suspected that this case will yield a higher thrust. Thrust was not calculated in the present study, but by considering the curves of the over pressure (blue) in figure 6 it is clear that the case with the lower equivalence ratio will have a larger contribution to the thrust when the integral of this over pressure over the front plate is considered. Finally, since the scales are the same in these two figures, the higher frequency in the case using the stoichiometric fuel/air mixture is immediately apparent.

Two different cases have been treated above, and by those two it is believed that it is the case with $\Phi = 0.6$ that best models the operation of the real engine. However, due to the complexities of the flow, and the many approximations introduced when transforming the problem to one that can be solved on the computer it is nigh impossible to know how accurate the simulations are. The following could be done in order to elucidate the situation:

- Redo the simulations with a higher resolution.

ANALYSIS OF THE OPERATION OF THE PULSEJET ENGINE

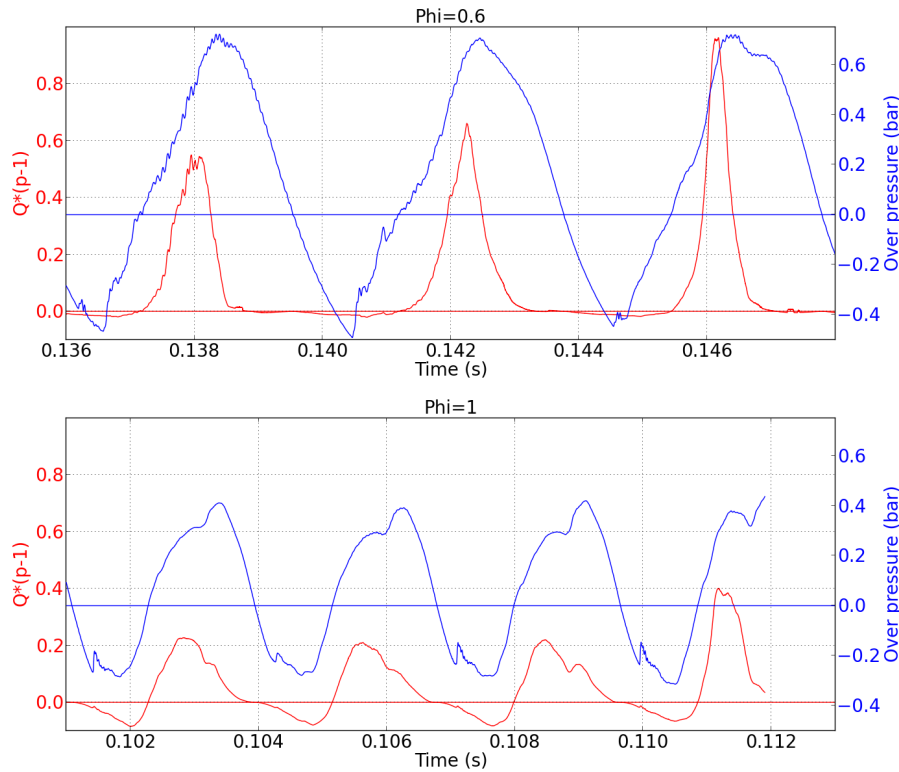


Figure 6 – Curves illustrating the overpressure at the front plate, and the product of this overpressure times the heat release for different equivalence ratios.

- Use a more detailed kinetic scheme.
- Use a better method to handle the flapper valves, instead of the boundary condition used to model the valve in the present study.
- Instead of only treating one tenth of the whole engine, include the complete engine, with all ten valves explicitly modeled.
- Extend the simulation to include heat transfer to, from and in the parts of the engine.

Although interesting and well worth considering, the points above all would require a lot of work and are not pursued further in this report. But since the integrated results of the simulations with $\Phi = 0.6$ agrees reasonably well with those for experiments in the literature the present simulations are deemed to be sufficiently accurate. And the results will be used to illustrate important events in the engine. To that end color plots at a slice through the center of the computational domain for four variables:

- Mach number, figure 7,
- Pressure, figure 8,
- Temperature, figure 9,
- Velocity in the axial direction, figure 10,

are displayed for one representative pulse. This specific pulse covers the time interval from $t=0.1403$ to $t=0.1446$. This interval is chosen such that this pulse starts and ends when the pressure in the combustor is around its minimum value, and are marked with red dots at the bottom of figure 4. It is also at these times that the velocity of the fuel/air mixture injected in the engine is at its maximum. Due to the pulsating character and the complex flow field it is a challenge to visualize the events going

on. Here the time interval under consideration is divided into 60 time steps, and plots are generated for each of these time step. In order to better discern what is going on, an adjustable color scale is used for all variables except for the Mach number. For the Mach number the range is fixed between 0 and 1 – and the reason for this is that by doing so the choked flow at the exit can be easily detected. Also, due to the large number of plots the figures from each individual time step have to be quite small, and, due to the large number of them the aggregated figures occupy a complete page each. The color plots from the different time steps are laid out so that the first time step is placed at the top of the left column and the consecutive time steps are placed below until the bottom of the left column is reached after which the next time step is placed at the top of the right column with the consecutive ones following below (in the right column). In order to be able to discuss individual figures, the rows 1, 5, 10, 15, 20, 25 and 30 are marked in each figure. Note also that in these color plots a large part of the external domain has been excluded.

Some events are easier to observe through a specific variable, and specific references will be given in the itemized descriptions below.

- The chosen time interval starts with the pressure in the combustor being well below ambient, the valve is open at its maximum, and a cold mixture of fuel and air is injected into the engine. From the plots of the axial velocity one can see a rather high velocity of the injected fuel/air mixture: about 150 m/s as indicated by the dark red color, e.g., in second row of the first column. This inflow leads to some kind of vortical structure, where the flow is directed towards the front plate at the center of the engine. Note also – as seen in the color bar – that the blue color represent a rather high negative velocity (to the left in the figure). The first and second row in the first column of the axial velocity further show how the compression wave from the previous pulse enters the combustor.
- The “visualizing slice” is cut through the center plane of the computational domain, and by doing so it also cuts through the center of the circular inlet. And both in the plots of the temperature and of the axial velocity the extension of the inlet valve can be discerned.
- The cold reactants flowing into the combustor develop a “mushroom” shaped structure, as can be seen in the first five rows in the left column for the temperature.
- At this time the pressure is low, but the temperature of the products in the combustor from the previous pulse is still high, e.g., the first five rows in the left column for the temperature. This is important to reflect over, since from an efficiency aspect one does not want a large fraction of the fuel to burn at this pressure below ambient. Furthermore, the Rayleigh criterion dictates that if more than a small fraction of the fuel is consumed at this low pressure, the pulsations are at risk to fade out.
- At the time when the inflow is at its maximum speed (when the pressure is at its minimum) a weak compression wave, developed under the previous pulse, and propagating upstream from the end of the engine is entering the combustor (as already mentioned under the first bullet). Considering row 1 to 10 in the left column for the pressure it can be seen how this compression wave becomes weaker as it enters the combustor (since it is entering an expanding volume). The reflection of this compression wave can also be seen, and it becomes more pronounced when it leaves the combustor and enters the tail pipe, something which can be seen in row 7 (in the left column). And the consecutive plots show the continued propagation of the compression wave towards the exit of the engine.

The effect of this compression wave on the pressure reading on the probe is also visible for both cases depicted in figure 6.

At the time when the pressure is at its minimum– (corresponding to the two first color plots, the two top ones in the left column), when the compression wave leaves the tail pipe, and enters the expanding section leading to the combustor – the plots in figure 10 illustrating the axial velocity show that the flow in the tailpipe is directed towards the open end of the engine, and still at a quite high velocity. But only after a few time steps, it can be seen how the flow changes

direction, and instead starts flowing towards the front of the engine. This is clearly seen in row 6 (left column) where the dark blue color indicates a velocity of around 170 m/s directed towards the front of the engine (to the left). This is a manifestation of the inertial effects, following the pulsating nature of the process, and precedes the build up of pressure in the combustor.

- The compression wave – and its refraction – can be seen to reach and pass over the plume of fuel/air flowing in to the engine on row 3 to 6 (left column). Now, the compression wave is rather weak, but by looking at the color plot of the temperature for the relevant rows the character of the structure of the fuel/air plume can be seen to have changed slightly. There will also be a slight increase in temperature following the passage of the compression wave. This increase is too small to induce any noticeable reactions – something which would anyhow not be desirable, since the pressure in the combustor at this time is too low to lead to efficient combustion.
- At a later time the inertial effects of the pulsating character of the combustion lead to an increase in pressure. This inertial effect will also be illustrated in figure 12 where the red curve shows the pressure at the front plate when the combustion was turned off.

The reactants introduced in the combustor will mix with the products from the previous pulse. Eventually the reactants will ignite at the interface with the hot products. Due to the distributed character of the burning surfaces, the pressure in the combustor starts to build up. If the combustion is sufficiently fast, or if the area difference between the combustor and the tail pipe is sufficiently large, a compression wave – travelling towards the exit of the engine – and a train of rarefaction waves – traveling towards the front plate – will develop. Neither of these are however visible in the figures below, indicating that the combustion is not fast enough for a clear compression wave to develop. But what can be seen is that a rather high pressure, about 1.7 bar, is reached in the combustor and in a rather large part of the tail pipe at the time corresponding to the color plot displayed in row 28 (left column). For the pressure it can also be noted that except for the time corresponding to the color plots in the first 17 rows in the left column the pressure in the combustor is fairly homogeneous.

- Some time after the maximum pressure has been reached in the combustor, the flow at the exit becomes choked. This can be seen in the color plots for the Mach number in row 5 to 11 in the right column, where the Mach number is larger than one in parts of the flow field in the flare. When the choked flow in the exit has been “relaxed away” a compression wave can be seen to emerge from the exit, and travel upstream toward the front of the engine, clearly seen in the color plots of the pressure, from row 15 and down in the right column. This compression wave is a consequence of the rarefaction waves mentioned above; when these hit the front plate, they are again reflected as rarefaction waves. However, when these in turn reach the open end of the engine the reflections will instead result in a compression wave propagating towards the front of the engine. At the same time as this happens, it can be seen how the pressure in the combustor is reduced, and eventually how fresh reactants are started to flow in (something which is easily observed in the plots of the temperature).
- It can also be seen – from plots of the axial velocity – how the compression wave traveling upstream has to do so against a rather high velocity. Compare for example the color plots of pressure and axial velocity at row 20 in the right column. The compression wave is well defined in both pressure and axial velocity, and from the latter it can be seen that it propagates against a velocity of around 470 m/s. So although the speed of this compression wave is supersonic relative to the medium in which it propagates, its velocity relative to the engine is significantly lower. Regarding the situation at this time, it should be noted that the temperature is elevated in the tail pipe, and consequently so is the speed of sound.

After considering the events in one pulse of the pulsejet engine, as demonstrated through the results from these simulations, it seems obvious that the most difficult issue to resolve when designing an efficient pulsejet are the contradicting demands posed on the combustion process in the engine:

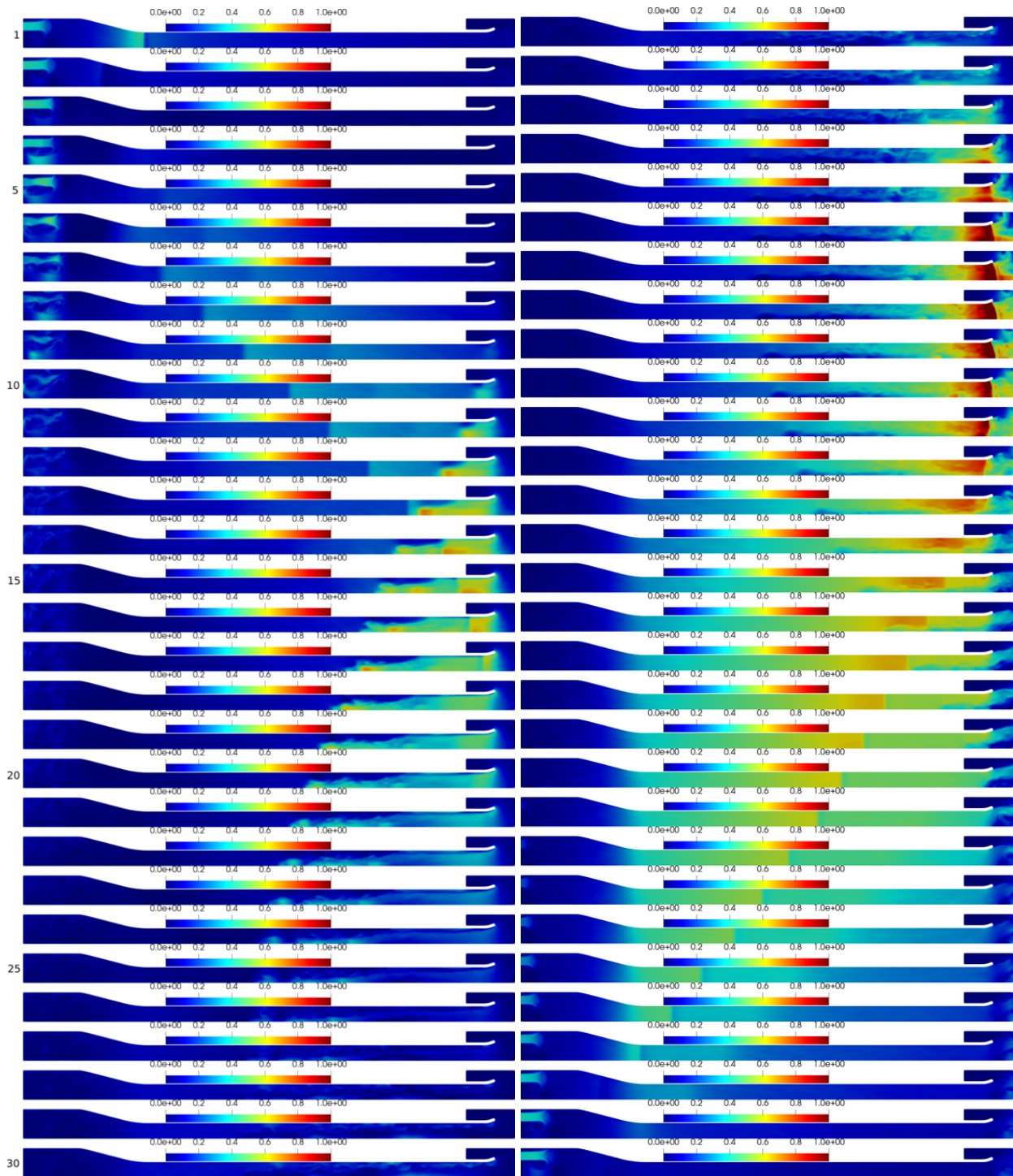


Figure 7 – Mach number.

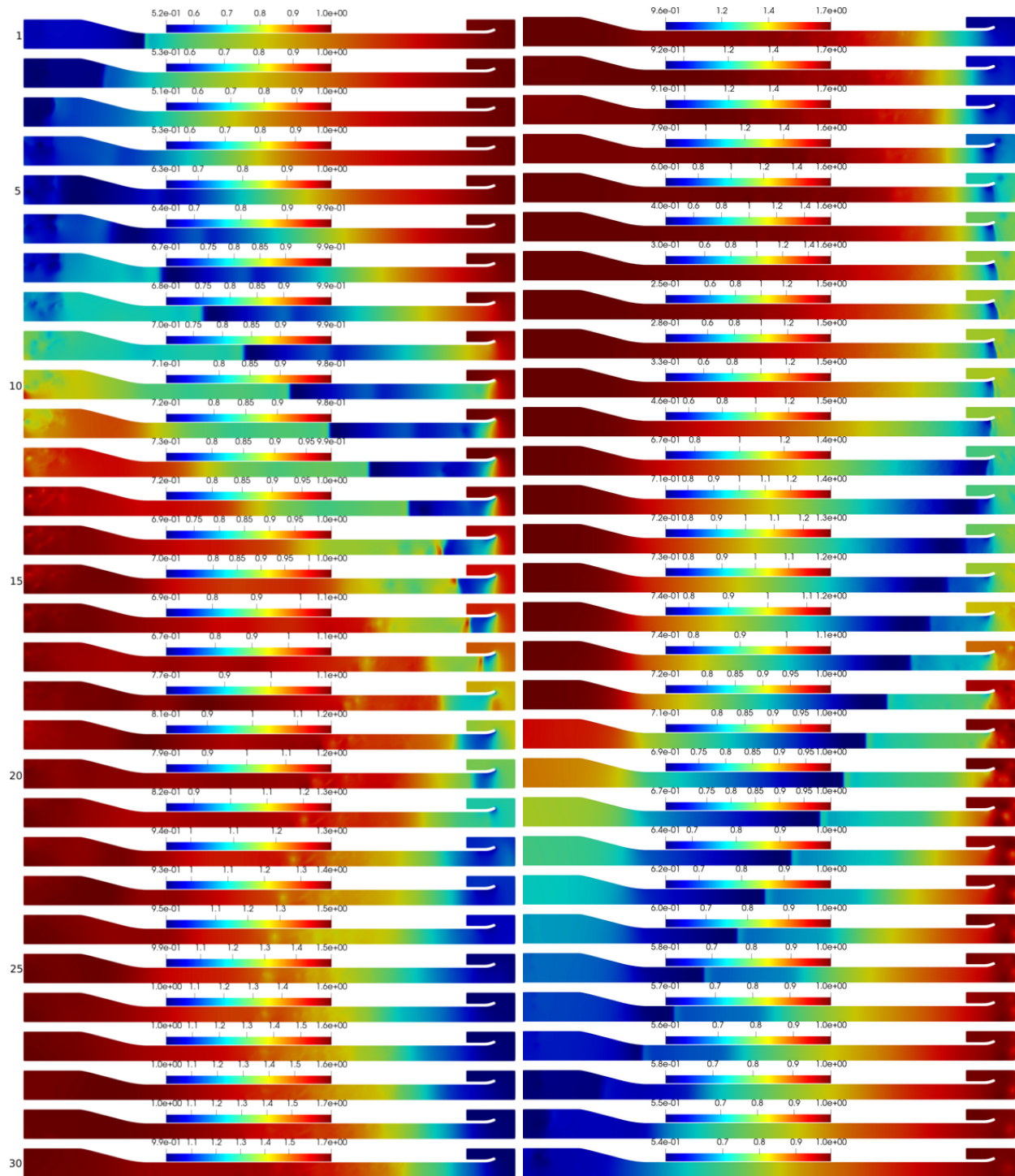


Figure 8 – Pressure.

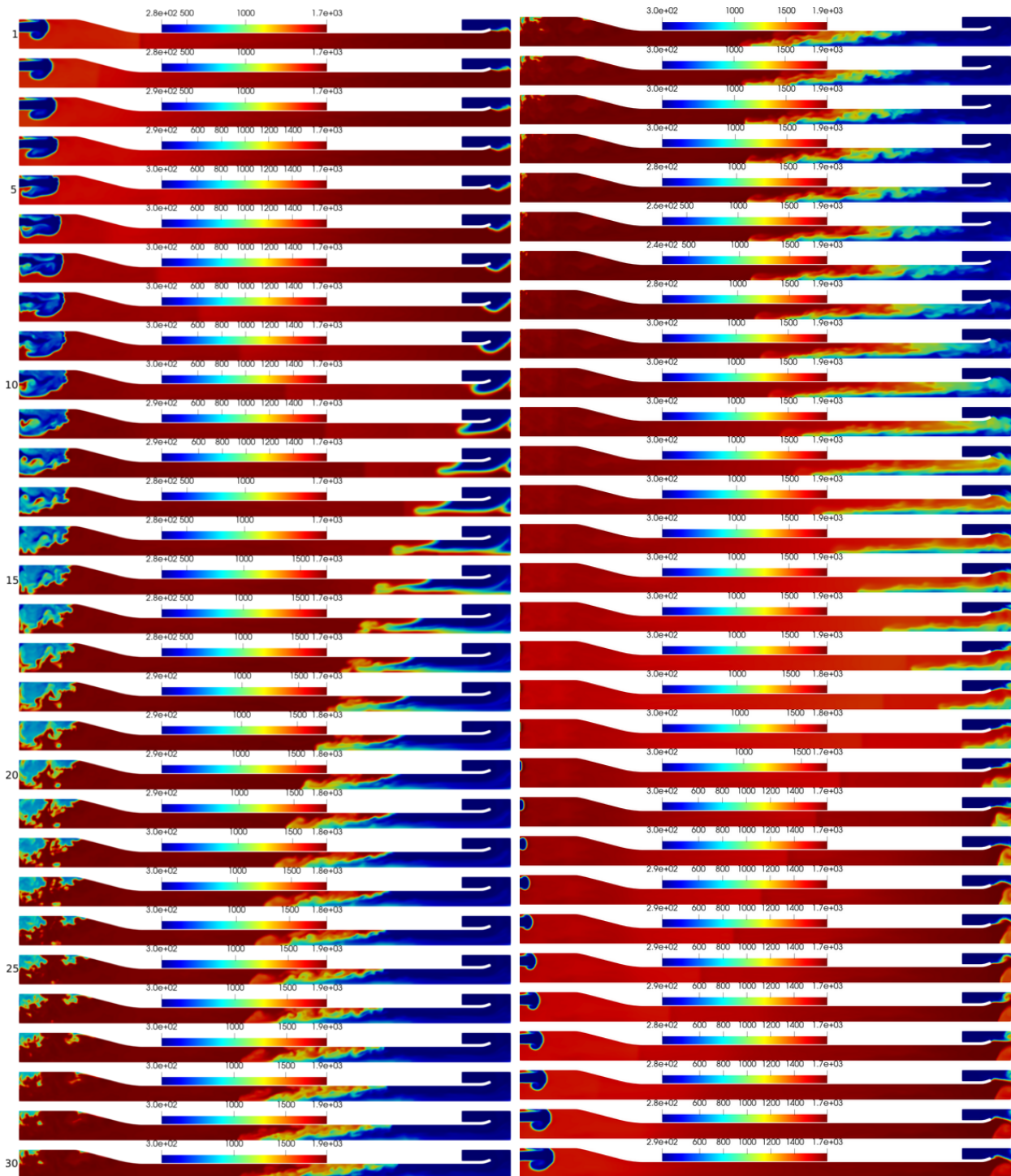


Figure 9 – Temperature.

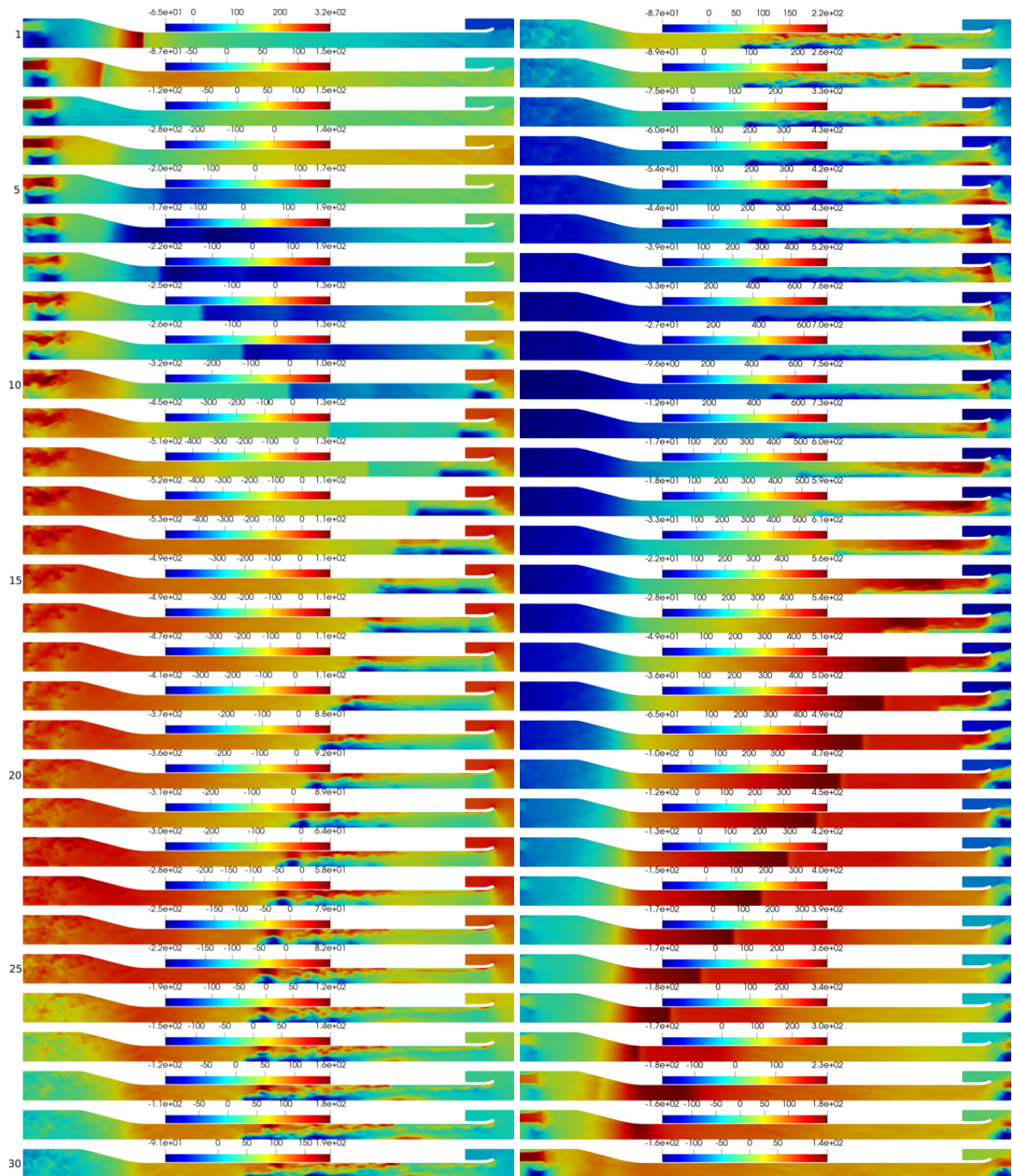


Figure 10 – Axial velocity.

1. In order to reach a high pressure in the combustor, the combustion has to be very fast. If not, the pressure will be relaxed through the tail pipe, and no or little thrust is generated.
2. Due to the way the valves operate, reactants are introduced into the combustor at a low pressure, and when this happens the combustor are filled with hot gases from the previous pulse. *If* more than a small fraction of the reactants are consumed at this point in the cycle, the performance of the engine will be lost, or the pulsations will fade out. So, contrary to the demand in the point above, in order to prevent this from happening the demand here is that the combustion should be delayed, so that it can start at a more profitable time, when the pressure has increased.

So in essence, the combustion should be *fast and slow* at the same time! The reaction of the major part of the fuel/air mixture should be delayed until the pressure has – due to the inertial effects of the pulsating combustion – increased to a level which both gives a level of compression adequate for efficient combustion and fulfilling the Rayleigh condition so that the pulsations does not fade out. And when it finally burns, it should do so as fast as possible for maximum performance.

This reasoning could also serve as an explanation of the behavior seen in this study, when a reduction of the equivalence ratio of the fuel/air mixture improved the general operation of the engine – most notably manifested by increased values on peak pressure. This is also clearly illustrated in the curves depicted in figure 6 where it is seen that a larger portion of the fuel is consumed at a low pressure for the stoichiometric case when compared with the leaner case, $\Phi = 0.6$.

To further elucidate the processes in the engine iso surfaces of the fuel and of the heat release – as well as color plots of Mach number and axial velocity through a slice through the center of the engine are presented in figure 11. In this figure only the combustor, and a smaller part of the tail pipe are considered. The four different variables in this figure are displayed at 6 different time steps, and similar to before they are ordered left top to left bottom, followed by right top to right bottom. All of the events in figure 11 corresponds to events in the left columns in figures 7-10, and the number (from the set of numbers 4, 8, 12, 16, 20, 24) displayed next to each batch of plots in figure 11 corresponds to the number in those figures above.

The most important feature obtained from these figures is the change in character during the time considered; at first the burning (as illustrated by the smooth iso surfaces for the heat release) is confined to a rather smooth surface, but later the burning is changed to a much more convoluted structure as seen in the last frame. This indicates that the burning surface dramatically increased during this process, and serve as an explanation of the fast combustion seen in a pulsejet. And the concept of “pressure gain combustion” in this context can in this case partially be explained by an extremely enlarged burning surface.

The difference in character of the iso surface of the heat release (mimicking the burning surface) between the first and the last plot illustrates the requirements of successful operation of the pulsejet: at first, when the fuel/air mixture is introduced combustion should be kept at a minimum (manifested by a smooth, comparably small burning surface), later on, when the pressure has increased it is instead advantageous if the combustion is as fast as possible (something which is here achieved by the very enlarged burning surface). It is also evident that it is going to be extremely difficult to design an engine where the level of intensity of the combustion is governed by a process as the one identified here.

As mentioned previously, there are several aspects of the simulation that could be improved (notably an improved model for the chemical kinetic and a higher resolution), however, in the light that the current simulation reasonably well reproduces the integrated results seen in experiments (frequency and peak pressure) it is believed that the current simulation is capable of modeling the important processes in the pulsejet.

In order to illustrate the pulsating character of the process, and how it is influenced by the combustion figure 12 is presented. In this figure pressure data from the probe next to the front plate (the same as used previously) for the same time interval used in figures 7-10 are presented. The red curve represent the pressure when combustion has been switched off in the simulations, and the blue is the result from the standard simulation, with combustion turned on. It is obvious that oscillations will

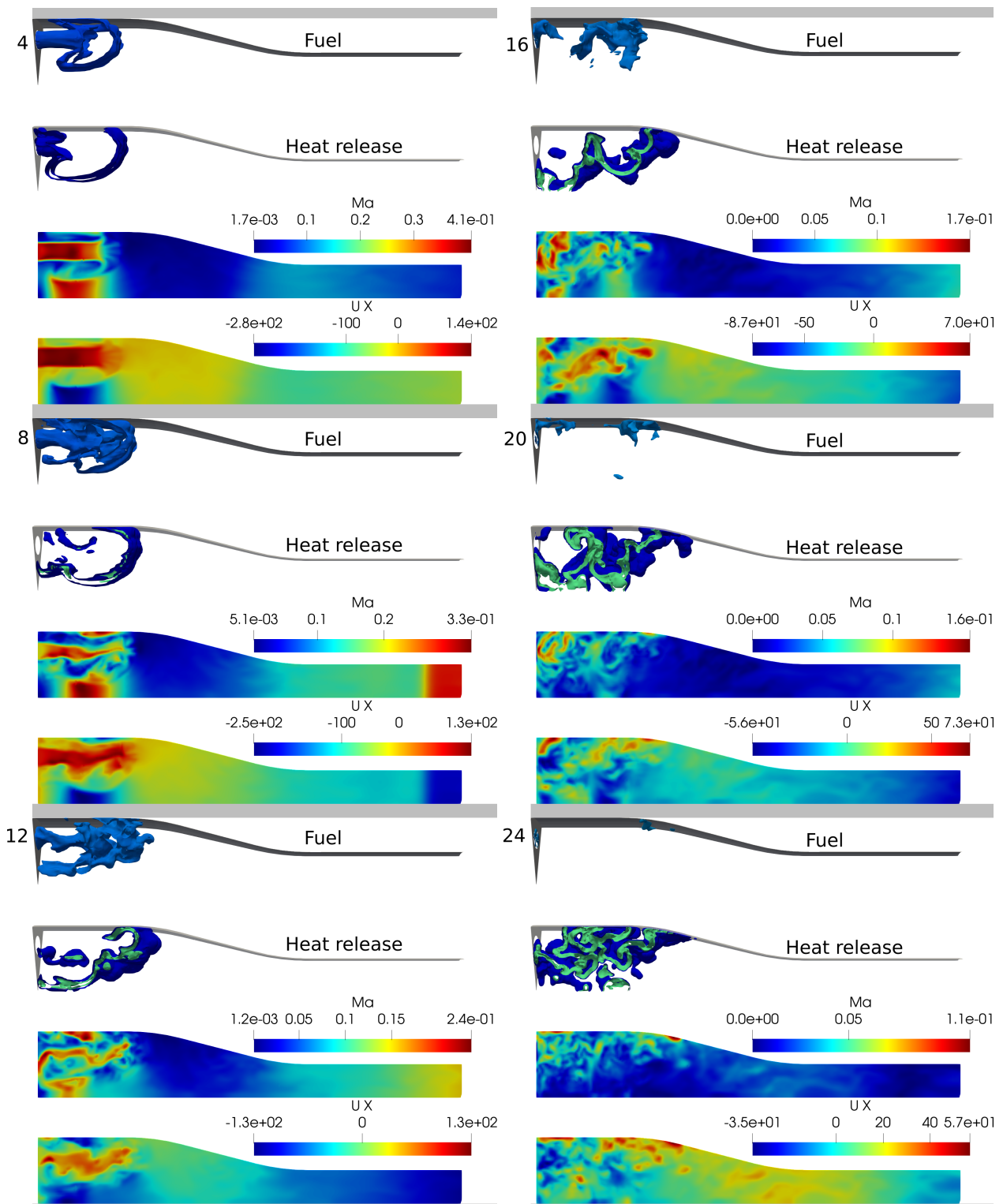


Figure 11 – Iso surfaces of fuel and heat release, and color plots of Mach number and axial velocity in a slice through the center of the engine. Data from six different time steps are displayed, with numbers in the figure (4, 8, 12, 16, 20, 24) corresponding to the numbers used in figures 7-10, i.e., the plots in the top left position corresponds to row 4 in in the left column in those figures, and the bottom right corresponds to row 24, also in the left column.

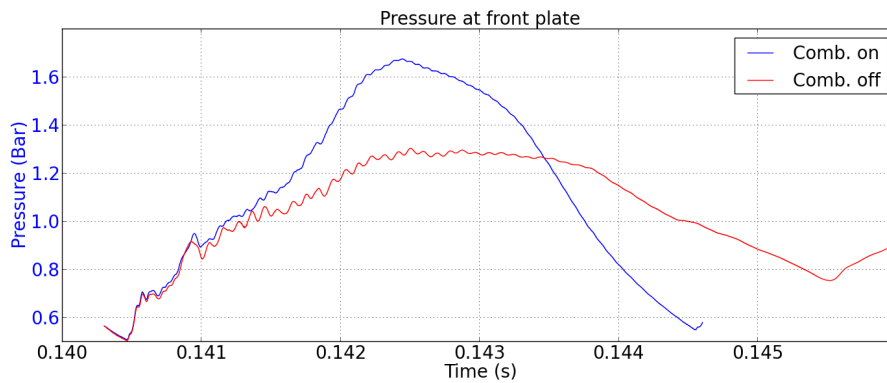


Figure 12 – With and without combustion.

eventually fade away when there is no energy input (in the form of fuel), but some observations can be made:

- At the beginning of the considered time interval the two curves follow each other closely, but start to diverge from each other as the effect of combustion have an influence on the pressure.
- In spite of the absence of combustion a rather high peak value is obtained, around 1.3 bar.
- The minimum value following the peak is not as low and occurs later than what was the case when the combustion was on. When there is no combustion the temperature in the engine will be lower, and consequently the speed of sound will also be reduced, which to some extent explains the longer period observed.

The red curve in figure 12 – the one resulting from the simulations when combustion was turned off – can in some sense be considered to illustrate a similar effect as seen in an Otto engine. And for the same reason as in an Otto cycle it is desirable that the major part of the combustion occurs at the time when the mixture has been compressed as much as possible. In an Otto engine this is readily achieved by firing the spark plug at the desired moment. In the pulsejet on the other hand this kind of direct control of the combustion process is lacking, and instead one has to rely on more indirect means; such as:

- Type and equivalence ratio of the fuel, and whether the fuel is liquid or in gaseous form.
- Number and type of injectors – as well as pressure in the fuel tanks, influencing among other things the droplet size, atomization, penetration length and turbulence level of the injected jets.
- Internal design of the engine, e.g., turbulence generators and flame holders.
- Whether or not active cooling is employed can also have an effect.

Obviously it is significantly more difficult to achieve an optimum timing of the combustion in a pulsejet compared to an Otto engine. Since in a pulsejet the equivalent of the “piston” in the Otto cycle consists of hot products from the previous pulse there is also a high risk for the combustion to begin *before* a desirable compression level has been achieved.

As was already illustrated in figure 6 there is a significant reduction of the peak pressure – and thereby on the performance of the engine – if the combustion starts “too early” (where in that case the differences were attributed to the different equivalence ratios in the two cases).

In an effort to illustrate the effect of the timing of the combustion idealized methods to model both the *mixing* and the *combustion* were used to evaluate the effect on the pressure. That is, idealized calculations were employed to illustrate the difference between combustion occurring early in the “compression phase”, or late, when a higher pressure has been built up.

This analysis was based on the following:

Initial data				Initial composition				
Case	Time (s)	p_0	T_0	CO=0.01	CO ₂ =0.11	H ₂ O=0.06	O ₂ =0.09	N ₂ =0.73
1	0.1404	0.523	1420					
2	0.1408	0.751	1530					
3	0.1414	1.003	1610					
4	0.1425	1.305	1760					

Table 1 – Initial data for idealized combustion analysis. p_0 and T_0 are pressure and temperature at the specified time from the simulation without combustion. Units are bar and Kelvin, composition show mass fractions.

- Based on the data represented by the red curve in figure 12 four different states were chosen to be used as initial data in the analysis, listed in table 1. In this table the actual time for the different states are displayed, as are the extracted values of pressure and temperature at these times. Also given is the composition of the mixture, and this is assumed to be the same for all four cases. It should be noted that there is a certain amount of uncertainty when identifying these values, but the important point in this analysis is the relative difference between the cases. Note also that what is considered “initial data” here essentially are conditions including products from the previous pulse.
- The same states for the injected fuel/air mixture as used in the simulations were used; i.e., 1 bar, 300 K, and two different equivalence numbers were used, 0.6 and 0.8.
- By looking at illustrations in figure 11 it is realized that the combustion process will be based on a combustor not completely filled with a fresh fuel/air mixture. And here it was assumed – somewhat arbitrarily – that the global mixture in the combustor consisted of either 30 or 40% (by weight) fresh fuel/air mixture, with the product from the previous pulse making up the rest. Again we argue that this arbitrariness is acceptable since we are mainly interested in the relative differences between the different cases. Furthermore, it was assumed that the two batches of gases (products and reactants) mixed ideally, something which was modelled by *Cantera*, [6].
- The actual combustion was assumed to occur instantly, and was modelled by a constant volume process, also implemented in *Cantera*. That is, the combustion process was modelled by first mixing the chosen amount of the cold reactants with remaining products from the previous pulse, and then calculating the states from a constant volume process applied to this mixture.

This obviously represents a dramatic idealization, but it do illustrate the effect of compression as is shown in tables 2. These tables display pressure and temperature for the different cases from this idealized calculation. The values with the subscript “mix” indicate the result from the mixing process, and p_1 and T_1 represent the results from the combustion process (applied to the mixture obtained in the previous step). In case 4 these idealized processes are applied at a time when the inherent compression is around its maximum value, and the values obtained can be said to represent the obtainable peak values in the engine. And depending on the combination of fill fraction and equivalence ratio the peak pressures for this case varies between 1.7 and 2.0 bar. The other cases represent combustion at earlier times in the compression cycle, and without further analysis the peak values in the engine for these cases cannot be estimated.

However, it would be reasonably straightforward to extend this analysis to do a more complete estimate of the pulsating operation, and a tentative strategy for achieving this is described in section 5.

4. Flame speed and its dependence on temperature

The pulsejet engine draws some of its characteristic traits from the fact that the fuel/air mixture is injected into a flow field filled with hot products from the previous pulse. These products contain highly reactive radicals, which are bound to have an influence on the reactivity of the fluid in those parts

Fill fraction=0.3, $\Phi = 0.6$					Fill fraction=0.4, $\Phi = 0.6$				
Case	p_{mix}	T_{mix}	p_1	T_1	Case	p_{mix}	T_{mix}	p_1	T_1
1	0.67	1100	1.0	1600	1	0.71	1000	1.2	1700
2	0.83	1200	1.2	1700	2	0.85	1100	1.4	1800
3	1.0	1200	1.4	1800	3	1.0	1100	1.6	1800
4	1.2	1400	1.7	1900	4	1.2	1200	1.9	1900

Fill fraction=0.3, $\Phi = 0.8$					Fill fraction=0.4, $\Phi = 0.8$				
Case	p_{mix}	T_{mix}	p_1	T_1	Case	p_{mix}	T_{mix}	p_1	T_1
1	0.67	1100	1.1	1800	1	0.71	1000	1.4	1900
2	0.83	1200	1.3	1900	2	0.85	1100	1.6	1900
3	1.0	1200	1.6	1900	3	1.0	1100	1.8	2000
4	1.2	1400	1.8	2000	4	1.2	1200	2.0	2100

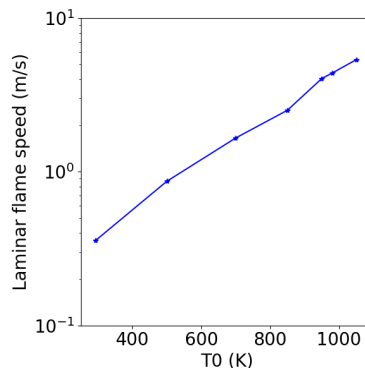
Table 2 – Results from idealized combustion. The subscript “mix” indicates the values obtained from the idealized mixing between the products and the reactants, and subscript “1” indicate the state obtained from the constant volume combustion. Units still bar and Kelvin.

where reactants and products do mix. However, as shown in [12] the most important influence stems from the elevated temperature. In an effort to better understand the effect of this elevated temperature its influence on the laminar flame speed was studied by doing one dimensional calculations of propagating flames with different temperatures on the unburned side.

The same code as already described was used in this case also (but obviously without turbulence modeling of any kind). The different temperatures at the unburned side used in the simulations, as well as the obtained flame speeds are shown in the table below:

T_0 (K)	293	700	850	950	980
s_L (m/s)	0.36	1.7	2.5	4.0	4.4

In these simulations a 42 step mechanism describing the burning of methane (CH_4) – initially stoichiometric – was used, and the pressure was set to 1 bar (note that previously propane has been used, the reason for using methane here was only to save time, since this code was already prepared with methane – the principal conclusion should however be the same with other fuels). Also, the fact that the heating in this study was assumed to occur under constant pressure (1 bar at all temperatures) means that the amount of fuel is reduced with increasing temperature (as is consequently the amount of energy that is released over the flame). The log plot of the flame speed below illustrates the exponential behaviour.



Curves illustrating the profile for the case with the lowest and the highest temperatures at the unburned side are shown in figure 13. The code uses an adaptable boundary condition on the velocity at the left end of the domain, and it is automatically adjusted so that the flame front should stay more or less fixed in the domain. As long as this is achieved (and the front does not leave the domain) the actual placement of the front is irrelevant. The important thing is instead the flame speed, and

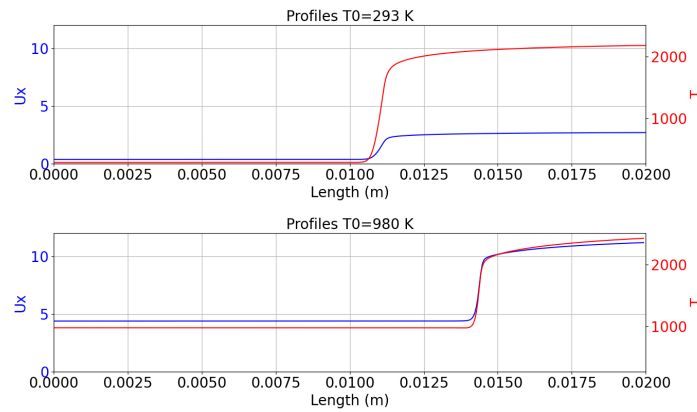


Figure 13 – Laminar flame profiles for two different temperatures at the unburned side. Units in m/s and K.

due to the adjustment of the velocity boundary condition, it can be directly read at the left end of the two curves. Note also that the same scales are used in this figure, and as can be seen the elevated temperature leads to a dramatic increase in the flame speed. It can also be noted that there is a substantially lower increase in the temperature over the flame for the “warm” case (in contrast to the behavior of the axial velocity, where the situation is reversed).

It is important to realize that at the elevated temperatures considered in this laminar flame study there is bound to be non-negligible reactions occurring at the unburned side. The reason for not observing this in the profiles is just a consequence of the comparably short residence time, and the scales used in the figures. One should also stress that it would be difficult to design an experiment with similar conditions as used in these simulations; the experiment would have to provide an inflow (at the left side) of the fuel/air mixture, and this mixture would have to be momentarily heated to the desired temperature at the inlet. However, it is not unlikely that in the violent conditions inside a pulsejet smaller domains are developed, where mixtures with similar conditions are obtained. Since the engine run extremely hot, these kinds of conditions can also not be excluded in the heated boundary layers, next to the heated inner parts of the engine.

Finally, the value of a study of laminar flames at elevated temperatures in this context is not because the combustion inside a pulsejet is believed to mainly occur in laminar form, it lies rather in the fact that the laminar flame speed has a direct effect on how, and how fast, a more turbulent combustion is developed. And the exponential behaviour on temperature is bound to have a profound effect on an engine like the pulsejet, where the fresh fuel/air mixture is injected and mixed with the hot products from the previous pulse.

5. Future work and a proposed strategy for performance analysis

In [10] a simplified method for estimating the performance of a pulsejet is presented. This thesis is from 1987, and therefore used less computationally demanding methods than what can be used today. However, the study is interesting in that it uses the method to first calibrate the method against experimental data from real engines and then employs it to evaluate the performance of a different injection method, Synchronous Injection Ignition, SII – and shows that this improved method of injection leads to a substantially improved performance.

The performance method uses quasi one dimensional non-steady, flow simulations (based on the method of characteristic). The combustion is modelled by combining two models; one using a zero-dimension perfectly stirred reactor, and the other using a one-dimensional mixing model. The model also incorporates empirical methods for including the effects of friction, atomization, mixing, injection and heat transfer. The heat release in the combustion model is based on (a fictitious?) flame speed, which is adapted in the calibration process.

Apart from a general description of the SII-method (pressurized inflow of fuel) it is unfortunately not described in any detail. One illustration indicates that the fuel valve is open for about one tenth of the

pulse (which is a lot less compared to the situation when using standard fuel injection), but nothing is written about the specific choice indicated in that illustration, specifically as to *when* and for *how long* in the pulse the fuel valve should be open. However, it is claimed that the improved performance is a result of the increased flow speed of the injected fuel; the increased flow speed leads to a reduced mean droplet size as well as larger penetration depth and better mixing which in turn is claimed to lead to more efficient combustion.

The most important conclusion from the work presented in [10] is the fact that it not only presents a calibrated performance model for the pulsejet, but also claims that this performance model can be used to favorably evaluate the performance using the Synchronous Injection Ignition method. It is further claimed that using this method – pressurized fuel injection during a shorter time frame, applied at a favorable time in the cycle – improves the performance of the pulsejet to a level where it is comparable to that of a turbojet engine.

However, since CFD tools have matured since the work described in [10] was done, a different performance model is proposed here. The proposed model is influenced by the findings described in this report. Instead of using the method of characteristic (as in [10]), it is here proposed to use standard CFD simulations, without explicitly including combustion in the simulation. The effect of the combustion is instead handled by using *Cantera* to calculate an estimate of the heat release (see section 3.above), and transfer this to the CFD simulation through a source term in the equation of energy. Here axisymmetric simulations are proposed, but if the geometry of the engine requires, it would be straightforward to use a general three dimensional model instead. In all, the following steps are required in the proposed performance model:

1. Provide important input data to the model:

- The equivalence ratio (φ).
- The amount of fuel introduced in each pulse. Here this is specified by introducing a *fill fraction*, $F_f = \frac{m_f}{m_T}$ where m_f is the mass of fuel/air injected and m_T is the mass of the fuel/air in the combustor under ambient conditions.
- The “speed of the combustion” has to be provided in this model, and it is given by Δt_c which specifies the time it takes for the combustion process to be completed. As pointed out in [10] this will have a large impact on the performance.
- The pulsating character of the process (obviously) leads to a highly varying pressure in the combustor, and an important parameter is *when* in the cycle the combustion is assumed to start. Here two different approaches are considered: (i) the combustion is assumed to start when the pressure in the combustor is at its lowest value, or: (ii) the combustion is assumed to be completed at the time when the peak value of the rebounding pressure in the combustor is reached, see e.g., the second peak in the curves in figure 14. In this figure the distance between the purple lines indicate the time interval under which the combustion occurs (Δt_c), and the first of them indicate when the modeled combustion starts. Other approaches are of course possible, but these two were considered based on the belief that the first one would be reasonable to use to model an existing pulsejet, and the second one seemed to be a good candidate to use for an “improved” pulsejet.

2. Initialize the process by setting estimated values on the states in the combustor. The simulations have previously used 2000 K and 1.4 bar in the combustor, and these values are used here as well.

3. In this step either *reactingFoamFOI* or *rhoCentralFoam* under the OpenFOAM framework are used to model the *effects* of the combustion (modeled using source terms in the equations, with data obtained from *Cantera*, see below). Here an axisymmetric model of the engine is used in the simulation, but it would be straightforward to instead use a full three dimensional model, only more time consuming. In order to get relevant data for the following iteration the simulations have to be long enough for the rebounding pressure to be captured (as seen for the two cases in figure 14). In all of the iterations, except the first the combustion will be modeled as a source

term of the heat release during the time interval the combustion is assumed to occur (Δt_c). The size of this source term is determined by data obtained from the previous iteration. In a similar way the mass of the injected fuel/air is also handled as a source term.

4. When the simulation in the step above is completed, the relevant states at the time when the following pulse is assumed to start are extracted (these states are used to provide initial values at the subsequent iteration, i.e., providing the states at $t = 0$ for the next iteration). Also, it is the mean values of the states in the combustor that are used in this and the following step.
5. Use the states obtained in point 4, and perform the idealized calculation of mixing and combustion – using *Cantera* as described previously. As a result of these simulations the heat release connected to the process can easily be extracted, and used in the next iteration.
6. Repeat from step 3, where the source term have been updated according to step 5.

This method was applied to same the engine that has been used previously in this study, and two specific cases were considered; one with “slow” combustion and one with “fast” combustion. In the case with the slow combustion the combustion was also assumed to start at the point in the cycle when the pressure was at its minimum. In the fast case, the combustion was instead assumed to start at a point in the cycle when the pressure was elevated, so that the combustion was finished at peak pressure.

The input data – as well as the obtained values on thrust, frequency, and specific impulse – for the slow case are given in the table below:

Slow combustion, at low pressure, $\Delta t_c = 0.0015$ s. $F_f = 1$ and $\phi = 1$.		
Thrust, 22 (N)	Frequency, 224 Hz	Specific impulse, 9600 m/s

In [5] it is reported that the thrust for this particular engine is 25 N, and that it operates at 232 Hz. So even if the method described above is rather crude, it gives surprisingly good agreement with experimental data.

The input data, as well as the results, for the case using the “fast combustion” are shown below:

Fast combustion, at higher pressure, $\Delta t_c = 0.0005$ s. $F_f = 0.5$ and $\phi = 0.6$.		
Thrust, 15 (N)	Frequency, 140 Hz	Specific impulse, 28000 m/s

The resulting pressure traces at the front plate for the two cases are shown in figure 14, with the slow case to the left. These curves are a result of the axisymmetric simulations described earlier, and it is important to understand that these simulations model the effect of the combustion, but that they only do so for the first of the pulses shown in the figure. So, for both of the cases the heat release take place when $0 \leq t \leq \Delta t_c$, and in the figure the time corresponding to $t = \Delta t_c$ are marked by a vertical red line. The first purple line indicate the time when the combustion is determined to start, based on the criteria used for the two different cases (the slow based on the minimum pressure, and the fast based on a specified time before the peak value). The second purple line indicates the time when the combustion is assumed to be completed. However, since this is part of an iterative process, there is no modeling of the combustion between the purple lines in the actual simulation, and basically the part of the simulation after the time determined by the first purple line is superfluous (however, for the fast case that time is determined based on when the rebounding pressure peak occurs).

That is, once the iterative process has converged, the pulse ends at the time determined by the first purple line, and then it repeats itself from $t = 0$ (it repeats itself in the *next* iteration, but once the method has converged the curves will be very similar between the iterations). Since the curves in the figure show a more or less converged solution, the part after the first purple line shows what would happen in the first pulse *after* the combustion is turned off. By comparing the curves between the purple lines with the part between y-axis and the red line one gets an illustration of the effect of the actual combustion. Also note from the curves that the frequency of the case with slow combustion is substantially higher than the case with fast combustion (also seen in the tables above) – something

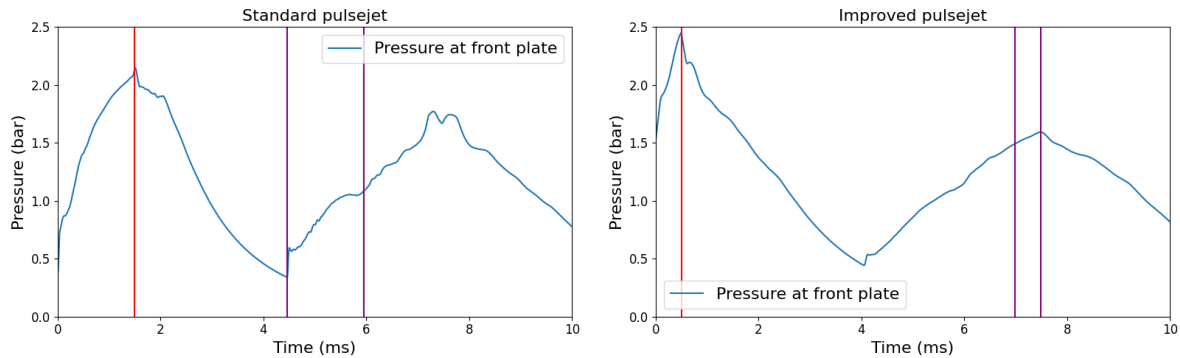


Figure 14 – Pressure on the front plate. Standard pulsejet with slower combustion, at a lower pressure to the left. Improved pulsejet with faster combustion, at a higher pressure to the right. The vertical lines are used to illustrate the time interval during which the combustion occurs. The combustion is “on” between $t = 0$ and the time marked by the red line (corresponding to Δt_c).

which is explained by the fact that a lot less fuel is used in the fast case, leading to a lower temperature in the engine, and hence a lower speed of sound.

The results presented above indicate that a dramatic increase in the specific impulse can be obtained if one has better control over how the combustion occurs. Translated to fuel consumption it indicates that the improved pulsejet has a fuel consumption of about one third of that of the original engine. The level of the specific impulse obtained even compare favorably to those of a generic turbojet engine, and thereby these preliminary results confirm the claim in [10].

The results are preliminary, but they do serve as a powerful motivation for continued study of these aspects of the pulsejet engine. In a future effort it is therefore proposed to undertake a systematic study of key parameters:

- The timing of the combustion.
- Type of fuel and the equivalence ratio of the fuel/air mixture.
- Fill fraction of the fuel/air mixture

It would also be important to study geometrical variations of the engine. For instance, in this scenario it is likely that a reduced area ratio between the combustor and the tail pipe (which is typically quite large for small engines) would be advantageous if the combustion can be controlled as outlined above.

Finally, the proposed performance model neglects all the details of the mixing of the fresh fuel/air mixture with the hot products from the previous pulse, as well as all the finer details in the combustion process. But even if it is difficult to have detailed control of the timing of the combustion in a real pulsejet engine, this method can be used to evaluate the *effect* of such a timing. Hence, in a first step it should be possible to use the method above to optimize both the geometry and the timing of the combustion in the engine. In a second step the goal would then be to implement these optimizations in a real engine.

6. Conclusions

Numerical simulations were used to model the operation of the commercially available RedHead pulsejet engine.

By reducing the equivalence number of the fuel/air mixture from 1 to 0.6 good agreement between results from the simulations with experimental data in the literature was obtained.

A large number of figures were presented, visualizing the important events in the engine. The study clearly identified the combustion as the “tricky” part when it comes to understanding the operation of the pulsejet. In particular it was noted that the numerical results showed that although the operation using a lean fuel/air mixture ($\Phi = 0.6$) showed good agreement with the experiment, the agreement –

as well as the performance – of the engine markedly deteriorated when a stoichiometric mixture was used. That is, the simulations essentially showed that an increased amount of fuel per pulse led to a reduced thrust.

Comparisons between the results using stoichiometric and lean fuel/air mixtures clearly showed that the reduced performance seen when the stoichiometric mixture was used could be explained by the fact that for this case – in contrast to the lean case – a large part of the combustion occurred at a phase in the pulse when the pressure in the combustor was below ambient.

It was generally noted that the requirement on the combustion in a pulsejet should be both “slow” and “fast”: it should be *slow* so that even (by design) the fuel is introduced at the “low pressure phase” of the cycle it should essentially not burn at that phase, and it should be *fast* so that when it finally burns (at a more elevated pressure) it should do so sufficiently fast so that it becomes close to a constant volume combustion process, resulting in as high pressure as possible in the combustor.

The operation of the pulsejet has some similarities with a Otto engine, but here the piston is replaced by a column of hot products, and similar to the Otto engine it is from a performance perspective desired that the bulk of the combustion occurs when the mixture has been compressed adequately. However, since the “piston” in the pulsejet consists of hot products, there is the challenge of preventing combustion in the low pressure phase, hence as noted above, the combustion should be “slow” initially.

Furthermore, visualizations of the burning surface in the combustor provided an explanation of how this “slow and fast” requirement could be achieved. It was noted that the burning surface at the beginning of the injection phase was smooth and not particularly folded, and that at a later phase the burning surface was highly convoluted, with a substantially larger total area than at the earlier phase. So the simulations of the specific case in this study indicated that the initial, “slow” combustion could in part be attributed to a small burning surface initially, and the later “fast” combustion could similarly be attributed to a substantially enlarged burning surface at a later time.

In this context it should finally be noted that from a design perspective it would be *extremely* difficult to design a “traditional” pulsejet where this “slow and fast” combustion is optimized since it depends on so many different aspects, e.g., turbulence, kind of fuel, type of injectors, internal structures of the engine, liquid or gaseous, cooling etc.

However, we do believe that the understanding of the important processes that this study has provided, as well as the experiences of the tools employed puts us in a unique situation where it could be hoped that more efficient designs of the pulsejet engine could be conceived.

For instance, in [10] it was shown that the performance could be dramatically increased by switching to a controlled injection of pressurized fuel, letting it enter faster, and at a time in the cycle when the pressure level then leads to a more efficient combustion. Furthermore, this kind of dramatic improvement of the engine was also captured by a performance model developed during the project behind this report.

Since the pulsejet is extremely simple (i.e., inexpensive) a more efficient version of it would indeed be highly attractive in many areas. If – as is also claimed in [10] – the performance of an improved pulsejet would rival that of a turbojet engine it is realized that such an improved technology would have a very big influence on a wide range of flying applications.

7. Copyright Statement

The authors confirm that they, and/or their company or organization, hold copyright on all of the original material included in this paper. The authors also confirm that they have obtained permission, from the copyright holder of any third party material included in this paper, to publish it as part of their paper. The authors confirm that they give permission, or have obtained permission from the copyright holder of this paper, for the publication and distribution of this paper as part of the ICAS proceedings or as individual off-prints from the proceedings.

References

- [1] Bressloff, N W. “A Parallel Pressure Implicit Splitting of Operators Algorithm Applied to Flows at all Speeds”. In: *Int. J. Num. Methods in Fluids* 36 (2001), p. 497.

- [2] Fedina, E, Fureby, C, Bulat, G, and Maier, W. "Assessment of Finite Rate Chemistry Large Eddy Simulation Combustion Models". In: *Flow, Turb. and Comb.* 99 (2017), p. 385.
- [3] Fureby, C. "A Comparative Study of Subgrid Models, Reaction Mechanisms and Combustion Models in LES of Supersonic Combustion". In: *AIAA 2019-4273* (2017).
- [4] Geng, T et al. "Combined Numerical and Experimental Investigation of a 15-Centimeter Valveless Pulsejet". In: *AIAA Journal of Propulsion and Power* 23.1 (2007), pp. 186–193.
- [5] Geng, T et al. "Combined Numerical and Experimental Investigation of a Hobby-Scale Pulsejet". In: *41st AIAA/ASME/SAE/ASEE Joint Propulsion Conference and Exhibit, 10-13 July 2005, Tuscon, Arizona* (2005).
- [6] Goodwin Dave, Malaya Nicholas, Moffat Harry, and Speth Raymond. *Cantera*. www.cantera.org. 2017.
- [7] Hairer, E and Wanner, G. *Solving Ordinary Differential Ordinary Differential Equations, II: Stiff and Differential-Algebraic Problems, 2:nd Ed.* Springer Verlag, 1991.
- [8] Kim, W and S, Menon. "An Unsteady Incompressible Navier-Stokes Solver for Large Eddy Simulation of Turbulent Flows". In: *Int. J. Num. Methods Fluids* 21 (1999), p. 983.
- [9] Sabelnikov, V and Fureby, C. "LES Combustion Modeling for High Re Flames using a Multi-Phase Analogy". In: *Comb. Flame* 160 (2013), p. 83.
- [10] Smith, Dudley. "The synchronous injection ignition valveless pulsejet". Order Number 8812834. PhD thesis. The University of Texas at Arlington, 1987.
- [11] Tanahashi, M, Fujimura, M, and Miiyauchi, T. "Coherent Fine Scale Eddies in Turbulent Premixed Flames". In: *Proc. Comb. Inst.* 28 (2000), p. 5729.
- [12] Tegnér, J K. "Numerical studies of initiations in preheated regions and possible implications to PDE and RDE". In: *AIAA-2019-3954* (2019).
- [13] Weller, H G, Tabor, G, Jasak, H, and Fureby, C. "A Tensorial Approach to CFD using Object Oriented Techniques". In: *Comp. in Physics* 12 (1997), p. 620.
- [14] Zettervall, N, Fureby, C, and Heimdal-Nilsson, E. "Small Skeletal Kinetic Mechanism for Kerosene Combustion". In: *Energy & Fuels* 30 (2016), p. 9801.
- [15] Zettervall, N, Nordin-Bates, K, Heimdal-Nilsson, E, and Fureby, C. "Large Eddy Simulation (LES) of a Premixed Bluff Body Stabilized Flame using Global and Skeletal Reaction Mechanisms". In: *Combustion and Flame* 179 (2015).

8. Acknowledgments

Owe Lyrsén and Erik Prisell are greatly acknowledged for help, support and valuable feedback in the work leading up to this report. Christer Fureby, Oskar Parmhed, Kristoffer Danel and Christian Ibron are also acknowledged for valuable input.